A constant temperature hot-wire anemometer

1987 J. Phys. E: Sci. Instrum. 20 311

(http://iopscience.iop.org/0022-3735/20/3/016)

J. Phys. E: Sci. Instrum. **20** (1987). Printed in the UK

A constant temperature hot-wire anemometer

I S Miller, D A Shah and R A Antonia
Department of Mechanical Engineering, University of Newcastle, NSW, 2308, Australia

Received 23 July 1985, in final form 21 March 1986

Abstract. A constant temperature anemometer is described which is designed to operate hot wires with diameters in the range 0.63–5 μm. A special feature of the design is the use of separate current sources to supply the different halves of the bridge. This feature eliminates the need for dynamic stability compensation, necessary for commercial constant temperature anemometers. The frequency response of the present circuit compares favourably with that of a commercial circuit. The probability density and spectral density functions of the longitudinal velocity fluctuation, obtained with wires of different diameters, are in good agreement with those obtained with a commercial circuit.

1. Introduction

The measurement of velocity fluctuations in turbulent flows is usually made with 5 μm diameter hot wires operated with constant temperature anemometers. Although a constant current anemometer is frequently used for the measurement of temperature fluctuations (using wires of diameter as small as 0.25 μm), its use for measuring velocity fluctuations has been somewhat limited. A major limitation arises from the 'static' and 'dynamic' non-linearities of the wire response and the generation of higher harmonics for turbulence levels larger than about 5% (Comte-Bellot 1976). Wyngaard and Lumley (1967) noted that for a constant current anemometer circuit, large velocity fluctuations cause appreciable fluctuations in the time constant of the wire itself. In particular, the non-linearity of the anemometer output can significantly affect the skewness and higher-order odd moments of the velocity fluctuation (Comte-Bellot 1976). In contrast, constant current operation provides better signal-to-noise ratio than constant temperature operation. For this reason, constant current operation has been preferred by some investigators for fine scale turbulence measurements (Kuo and Corrsin 1971, Frenkiel and Klebanoff 1975, Gagne 1980).

The accurate measurement of higher-order odd moments is of some importance in the study of coherent structures in various turbulent shear flows. For example, the skewness of the longitudinal velocity fluctuation u reflects contributions from sweep and ejection events that characterise the organised motion in wall-bounded flows. Also the accurate determination of higher-order moments of velocity derivatives is essential in understanding the dynamics of turbulence. For example, the skewness of the longitudinal velocity derivative represents the average rate of production of mean-square vorticity by vortex stretching. Reliable measurements of the skewness require that the tails of the probability density function are determined accurately. For these reasons, we have focused our attention on a constant temperature anemometer.

Commercial constant temperature circuits such as those of DISA and TSI are often, though not always, used. It is sometimes necessary, for example, where the spatial resolution of the hot wire is important, to use hot wires with relatively short lengths while maintaining a sufficiently large value for the length-to-diameter ratio (e.g. Champagne *et al* 1967). This latter constraint may require wires of diameter significantly smaller than 5 μm to be used. We have found that, although Pt wires of diameter = 1.2 μm can be operated with a commercial constant temperature circuit (e.g. DISA 55M10), significant effort is required to ensure dynamic balancing of the bridge. In the case of the 55M10 bridge, the procedure for balancing was followed, as outlined in the DISA 55M10 operating manual. The highest settings of the high frequency filter and bridge gain for which compensation of bridge oscillations could be achieved were first determined. However, even with these settings we found that oscillations in the bridge circuit could still occasionally be set up, leading to breakage of the wire. Increasing the overheat over a series of steps and carefully checking the dynamic response of the bridge after each step did not necessarily ensure trouble-free operation at the required overheat setting. It should also be noted that the relatively large resistance of a 0.63 μm wire ($\simeq 574\ \Omega\ \mathrm{mm}^{-1}$ for Pt–10% Rh Wollaston) would preclude the use of the DISA 55M10 bridge, at least in its present form. These considerations indicated the need for a constant temperature circuit which could be used relatively easily with wire diameters in the range 0.63–5 μm.

Section 2 of this note describes the design of the constant temperature circuit. In § 3 we present a brief comparison of the frequency response of this circuit with that for a DISA 55M10 constant temperature circuit. Also presented are comparisons for the probability density function (PDF) and spectrum of the longitudinal velocity fluctuation obtained with each circuit.

2. Circuit design

Standard constant temperature anemometer circuits use full bridge circuits with the servo amplifiers output applied to the bridge top. The equivalent circuit (figure 1(*a*)) shows the servo amplifier in a closed-loop system with inverting and non-inverting voltage shunt feedback. The closed-loop gain of such a system is given by (Millman and Halkias 1972)

$$R_{mf} = \frac{R_m}{1 + \beta R_m} \tag{1}$$

where R_m is the amplifier transresistance gain defined as the ratio of voltage output to the source input current without feedback and β is the feedback network reverse transmission factor defined as the ratio of current feedback to voltage output. Constant temperature anemometers require a high gain and a high frequency servo amplifier to follow the fast velocity fluctuations measured with the probe. These circuits are very susceptible to oscillations near their gain/bandwidth frequency, usually greater than 1 MHz, due to the amplifier input/output phase shift with falling high frequency gain. The condition for oscillation in the closed-loop amplifier (Millman and Halkias 1972) is

$$\beta R_m = 1 \tag{2}$$

when the amplifier phase shift is 180°. To preserve stability in such a closed-loop system, the positive loop gain, for all frequencies, must be less than one.

The condition for oscillation for both inverting and non-inverting voltage shunt feedback amplifiers (Millman and Halkias (1972) is

$$\beta R_m = \frac{-RA_v}{R + R'} = 1 \tag{3}$$

when the amplifier phase shift is 180°. In (3), A_v is the amplifier open-loop voltage gain, R is the probe or overheat balance

0022-3735/87/030311 + 04 $02.50

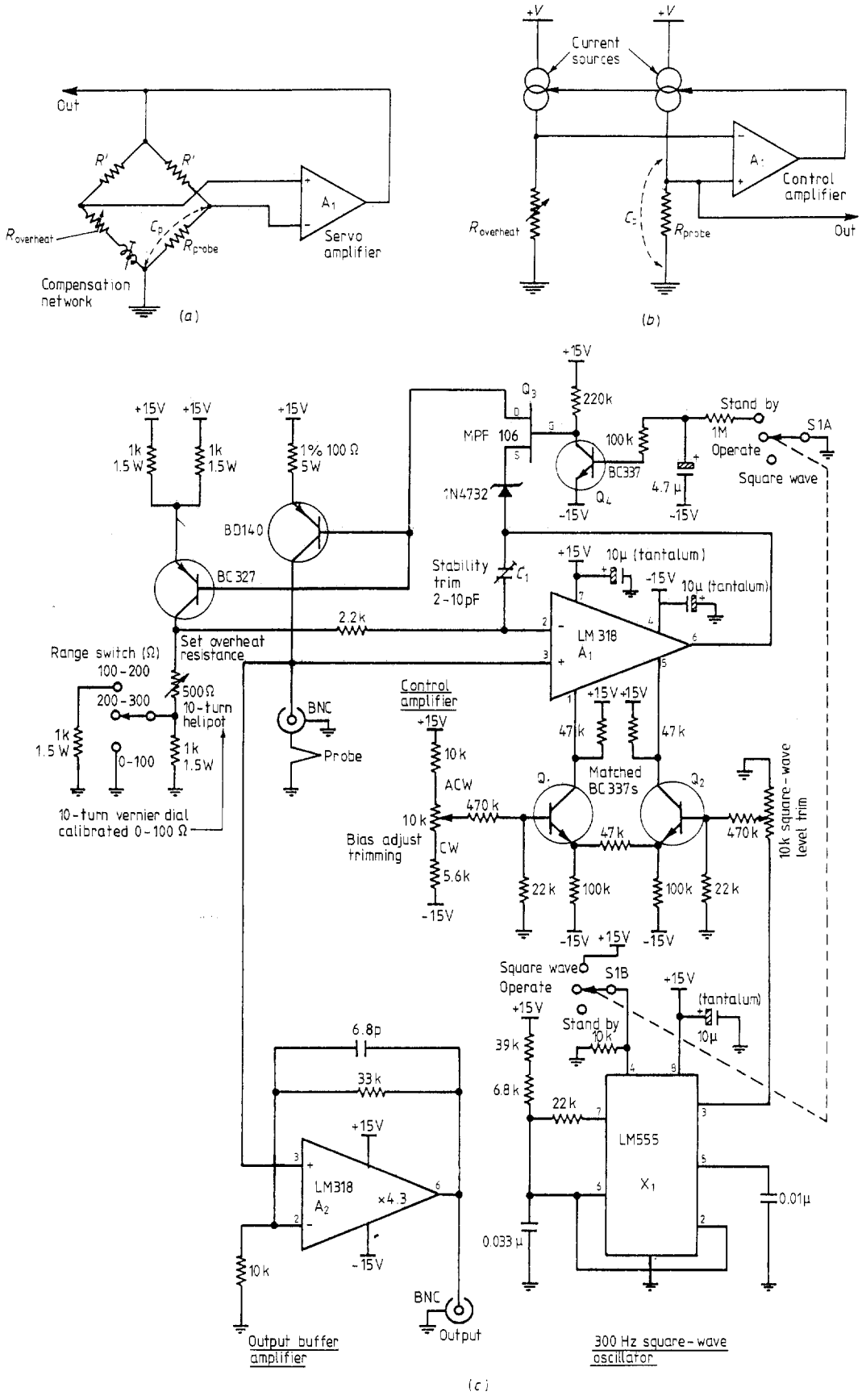

Figure 1. (*a*) Conventional bridge. (*b*) Current source driven bridge. (*c*) Constant temperature circuit.

resistance (figure 1(*a*)) and R' is the bridge top driving resistance for R (figure 1(*a*)). The amplifier gain A_v is a negative real number at low frequencies. However, the amplifier oscillations can occur at higher frequencies if $(R/R+R')|A_v|$ becomes unity when the phase shift of $-A_v$ is 180°. The situation is more critical with constant temperature anemometers, where the probe cable capacitance (C_p) causes extra phase shifts in the amplifier feedback circuit. Conventional circuits attempt to

compensate for these extra phase shifts by using dynamic compensation reactances in the balance leg of the bridge circuit (figure 1(*a*)).

The present circuit (figure 1((*b*)) was designed to remove the need for dynamic compensation adjustments. It is obvious from (3) that when R' is large, the stability of the amplifier can be greatly enhanced. For the present design, the bridge top resistors (R') have been replaced by two simple transistor current sources having theoretically infinite source resistance. The servo amplifier adjusts the current sources to heat the probe to the same resistance as the overheat balance resistance setting. Stable operation is now achieved without the need for dynamic compensation.

The full circuit diagram is shown in figure 1(*c*). In practice, the current source transistors are thermally linked to counteract temperature-induced drift. These two transistor types were selected for their complementary base/emitter voltage drop (V_{BE}) characteristics when used with the present bridge ratio (5:1). This particular selection assures close current source tracking during operation. The measurement of effective operating overheat temperature resistance shows very little variation ($\pm \frac{1}{2}\%$) with changes in air velocity from 0 to 14 m s^{-1} (table 1). This confirms the close current source tracking operation. The signal output is obtained from the buffer amplifier A_2 (gain = 4.3) fed from the active side of the probe. A small amount of high frequency roll-off above 1 MHz is applied to the servo amplifier A_1 by capacitor C_1. This precaution is included to ensure the stability of amplifier LM318 with different circuit layouts. A gain-matched pair of transistors Q_1–Q_2 feeds offset currents into the LM318 servo amplifier's balance inputs to provide bias adjustment and a square-wave test input from a square-wave generator X_1, at 300 Hz. Transistors Q_3–Q_4 provide gradual heating of the probe when the circuit is switched from 'standby' to 'operate'. A more accurate setting of overheat resistance can be achieved by using decade switch selectable overheat resistances instead of the calibrated vernier 10-turn potentiometer.

3. Comparison between present circuit and a DISA 55M10 circuit

The frequency response characteristics of the present circuit and a DISA 55M10 circuit were determined by examining the response of each circuit to a square-wave signal. The characteristic time τ_c for the probe/circuit combination was defined as the time taken for the magnitude of the output signal to decrease to 37% of its peak value. For the DISA circuit, the anemometer was adjusted at each flow velocity for optimum frequency response using the procedure outlined in the DISA 55M instruction manual. Measurements of the characteristic frequency $f_c(\equiv 1/2\,\pi\tau_c)$ were made for a 5 μm (Pt–10% Rh, 1 mm long) and a 1.2 μm (Pt, 0.25 mm long)

Table 1. Variation of overheat temperature resistance with air velocity for the present CTA (5 μm Pt–10% Rh, cold resistance = 10 Ω, overheat ratio = 1.6).

Velocity (m s^{-1})	Mean voltage drop across the probe (V)	Current through the probe (mA)	Effective overheat resistance (Ω)
0	0.52	32.01	16.24
0.6	0.57	35.24	16.17
1.4	0.62	38.04	16.30
2.5	0.65	40.29	16.13
3.8	0.68	42.23	16.10
5.2	0.71	43.82	16.20
7.1	0.74	45.59	16.23
9.9	0.77	47.48	16.22
11.0	0.78	48.30	16.15
14.0	0.80	49.04	16.31

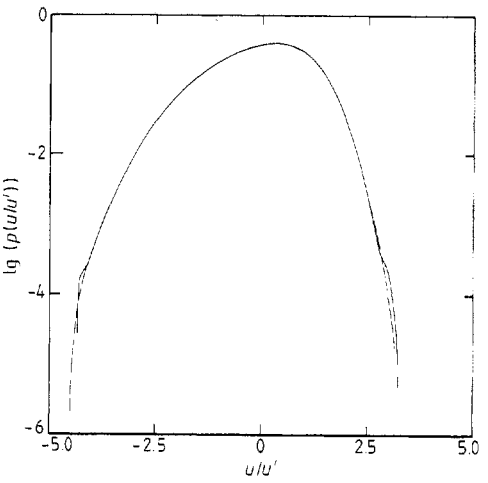

Figure 2. Probability density function of u obtained with the present circuit and with a DISA 55M10 circuit ($y/d = 0.5$, 1.2 μm wire). Full curve, present circuit; broken curve, DISA circuit.

Table 2. Comparison between normalised moments of u obtained with the present CTA and the DISA 55M10 unit.

d (μm)	y/d		u' (m s^{-1})	n = 3	4	5	6	7	8
5	0.3	Present	0.8768	−0.2266	2.736	−1.795	11.85	−14.11	69.88
		Disa 55M	0.87	−0.2026	2.704	−1.61	11.51	−12.67	66.36
	0.5	Present	0.7475	−0.4	2.936	−3.355	14.87	−29.0	108.6
		DISA 55M	0.7456	−0.3756	2.871	−3.029	13.75	−24.37	90.8
1.2	0.3	Present	0.9224	−0.2286	2.716	−1.741	11.45	−12.74	63.21
		DISA 55M	0.8767	−0.2553	2.769	−2.059	12.36	−16.66	76.4
	0.5	Present	0.7858	−0.4121	2.907	−3.385	14.5	−28.36	102.9
		DISA 55M	0.743	−0.4255	2.922	−3.465	14.49	−28.23	99.45

diameter hot wires (overheat ratio = 0.6) over a range of free stream velocities. For the present circuit, f_c varied between 11 and 16 kHz for the 5 μm diameter wire and between 50 and 65 kHz for the 1.2 μm diameter wire over the velocity range 1–15 m s^{-1}. These ranges of values compare favourably with the corresponding ranges of values obtained for the DISA circuit: 13–20 kHz for the 5 μm wire and 70–90 kHz for the 1.2 μm wire.

Measurements were made, using each circuit and the two previous hot wires, in a fully developed turbulent duct flow at a centre-line velocity U_0 of 12 m s^{-1}. The longitudinal velocity fluctuation u was obtained at $x/d = 2/5$ (x is measured from the duct entrance, d is the duct half-width) at two distances ($y/d = 0.3$ and 0.5) from the wall. The output from each circuit was conditioned using a buck-and-gain circuit and passed through a Krohn–Hite (model 3323) low-pass filter set at the Kolmogorov frequency $f_\eta (\equiv \bar{U}/2\pi\eta$, where $\bar{U}$ is the local mean velocity and η is the Kolmogorov length scale), which was approximately equal to 15 kHz at $y/d = 0.3$ and 0.5. The signal was then digitised at a sampling frequency of $2f_\eta$ into a PDP 11/34 computer. The digitised signal, of approximately 60 s duration, was linearised on the computer before processing the data.

Two statistics of u were considered: the PDF and the spectrum. The PDF contains information about the frequency of occurrence of particular amplitudes of the signal. The PDF p of u is normalised such that $\int_{-\infty}^{\infty} p\, \mathrm{d}(u/u') = 1$, where u' is the RMS value of u. To emphasise the tails of p, a semi-log presentation has been used in figure 2. It is not possible to discern differences between the two circuits, the ranges of p and $|u/u'|$ being nearly identical for the two circuits. Although the tails of the PDF exhibit a certain amount of scatter, the distributions in figure 2 indicate that the dynamic ranges of both circuits are adequate. Normalised moments $\overline{u^n}/u'^n$, derived from the PDF, are shown in table 2 for values as large as $n = 8$. The agreement between the circuits is good, at least up to $n = 6$. The scatter for $n = 7$ and $n = 8$ may be due to a lack of statistical convergence (Tennekes and Wyngaard 1972).

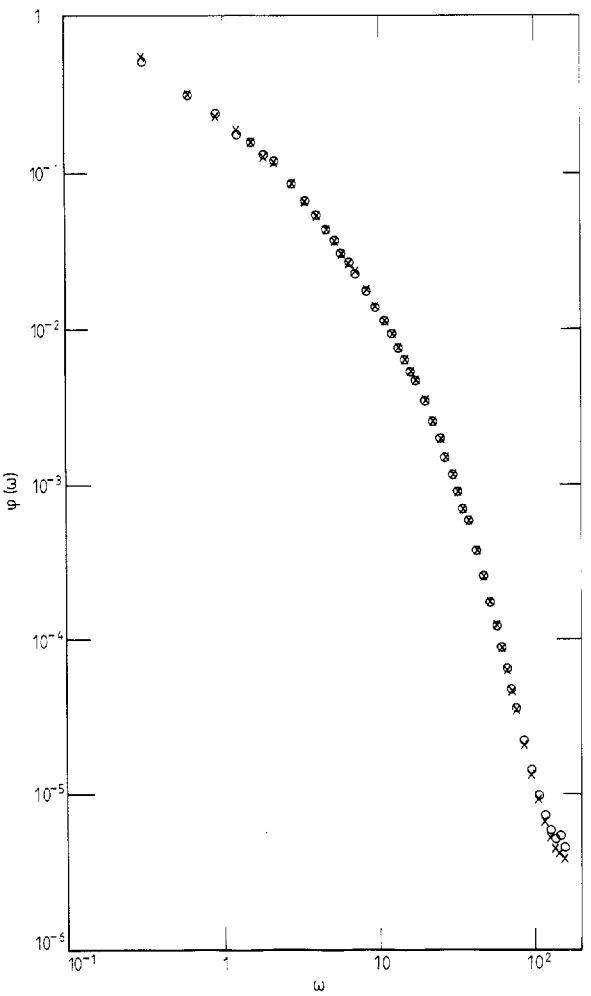

Figure 3. Spectrum of u obtained with the present circuit and with a DISA 55M10 circuit ($y/d = 0.5$, 1.2 μm wire). ×, present circuit; ○, DISA circuit.

The spectral density $\varphi(\omega)$ has been normalised such that $\int_0^\infty \varphi(\omega)\, \mathrm{d}\omega = 1$, where ω is the frequency normalised by U_0 and d ($= 2\pi f d/U_0$, f being the natural frequency). Distributions (figure 3) at $y/d = 0.5$ with $d = 1.2$ μm show that the agreement between the two circuits is good up to the Kolmogorov frequency. Similar agreement was obtained at $y/d = 0.3$.

The previous comparative results justify the performance of the present circuit. Since the cost of this circuit is less than AS$100, simultaneous measurements of velocity fluctuations at many points in space can be obtained very economically. Hot wires of relatively small diameter, e.g. 1.2 μm, can be operated in a stable manner with the present circuit.

Acknowledgment

The support of the Australian Research Grants Scheme is gratefully acknowledged.

References

Champagne F H, Sleicher C A and Wehrmann O H 1967
J. Fluid Mech. **28** 153

Comte-Bellot G 1976
Ann. Rev. Fluid Mech. **8** 209

Frenkiel F N and Klebanoff P S 1975
Boundary-Layer Meteorology **8** 173

Gagne Y 1980
Thèse Docteur-Ingénieur University of Grenoble

Kuo A Y-S and Corrsin S 1971
J. Fluid Mech. **50** 285

Millman J and Halkias C 1972
Integrated Electronics (McGraw-Hill: Kogakusha)

Tennekes H and Wyngaard J C 1972
J. Fluid Mech. **55** 93

Wyngaard J C and Lumley J L 1967
J. Sci. Instrum. **44** 363